

# Study on Tunnel Face Failure Mechanism in Two-Layer Soils

Tuan Anh Nguyen<sup>1</sup>, Minh Anh Trong Nguyen<sup>2</sup>

<sup>1</sup>Transportation Engineering Faculty, Ho Chi Minh City University of Transport, Vietnam

<sup>2</sup>Airports Corporation of Vietnam, No. 58 Truong Son St., Tan Binh District, Ho Chi Minh City, Viet Nam

## ABSTRACT

### Article Info

Volume 5, Issue 2

Page Number : 09-16

### Publication Issue :

March-April-2021

### Article History

Accepted : 01 March 2021

Published : 11 March 2021

Three-dimensional (3D) was not commonly used in the underground construction field as the stimulation process was quite complex and time-consuming. Recently, thanks to high precise calculator, the underground construction surveys by using 3D model gives more accurate results than that of 2D model. The reason is that 3D model represents not only all boundary conditions as theoretical models but also deformation area in two directions. Besides, it is possible for 3D model to analyse the tunnel stability and the balance pressure with the aim of ensuring the tunnel stability during the construction process. This article mentions the application of 3D finite element analysis on tunnel face failure mechanism and passive failure pressure in two-layer soils.

**Keywords :** FEM, Failure Mechanism, Passive Failure Pressure, Deformation, Tunnel Face

## I. INTRODUCTION

In recent years, developing countries have been experiencing a gradual urbanization. There are a growing lack of land, green spaces and public zones, whereas the population keeps a rapid increase. The consequences of problems are traffic jams, flooding, environmental pollution, etc., which makes the citizens more uncomfortable. Therefore, building the underground transport systems is critical in order to promote the pace of urban growth and improve the quality of people's lives.

The Earth Pressure Balance (EPB) Shield - TBM is currently the most ideal method for the tunnels construction at central cities. The disadvantage of this

method is that it puts active pressure on the ground before the excavation, which results in ground movement and impacts on surrounding constructions as well. Therefore, the study on the principles of pressure distribution and ground movement has great importance to support logically the construction work [8,11].

Over the decades, a number of researches have been carried out to investigate and calculate the active pressure on tunnel by using slurry and earth pressure balance shields in sand or clay [1-4,6,7,9,10,12-17]. However, the studies of the passive failure pressure on the tunnel and calculation on pressure are still not common. Therefore, it is critical and practical to conduct the studies on this issue.

This article focuses on analysing tunnel face failure mechanism and passive failure pressure in two-layer soils.

## II. METHODS AND MATERIAL

### A. Material parameters

Soil parameters for sand and clay and TBM is shown as Table I and Table II.

Table I. Geological Parameters

Soil parameters	Sand	Clay
Saturated unit weight, $\gamma_{sat}$ (kN/m <sup>3</sup> )	20.3	21.1
Unsaturated unit weight, $\gamma_{unsat}$ (kN/m <sup>3</sup> )	19.5	20
Cohesion intercept, $c'$ (kPa)	1.0	300
Angle of friction, $\phi$ (degree)	30°	1
Angle of dilation, $\psi$ (degree)	0	0
Secant modulus, $E_{50}$ (MPa)	27	100
Unloading and reloading modulus, $E_{ur}$ (MPa)	81	300
Oedometer modulus, $E_{oed}$ (MPa)	27	100
Poisson's ratio, $\nu'$	0.3	0.3
m	0.5	1.0
$R_f$	0.9	

TABLE III. PARAMETERS OF TBM SHIELD

Parameter s	Symbol	Value	Unit	Formula
Type of Behaviour	Material	Elastic	-	
Thickness	$t_c$	0.35	m	
The cross-sectional area of 1m length	A	0.35	m <sup>2</sup>	
Moment of inertia	I	$\frac{0.0035}{8}$	m <sup>4</sup>	$I = \frac{t_c^3 \cdot 1}{12}$

Density of concrete	$\gamma_c$	25	kN/m <sup>3</sup>	
Modulus of elasticity	E	23.5x10 <sup>6</sup>	kPa	
Stiffness	EA	8.2x10 <sup>6</sup>	kN/m	
Flexural rigidity	EI	8.4x10 <sup>4</sup>	kNm <sup>2</sup> /m	
Equivalent thickness	d	0.35	m	$d = \sqrt{12 \frac{EI}{EA}}$
Weight	W	38.150	kN/m/m	

### B. Analysis

The tunnel with the 5m diameter is stimulated for cases with C/D ratio of 1.5; 2.0; 2.5; 3.3 and 4.0 respectively by using PLAXIS 3D TUNNEL software [5].

Due to symmetry, only a half of the tunnel was stimulated in this model. The model extended 20m in the z-direction, with the width and depth of 30m and 50.5m respectively. This model is large enough to allow any collapse mechanism to evolve and avoid significantly influence on the boundary of the model. The interaction between the TBM and soil is defined by the boundary. During excavation, the tunnel pressure is put in the z-direction.

Geometrical configuration of stability model is illustrated in Fig. 1 (a,b).

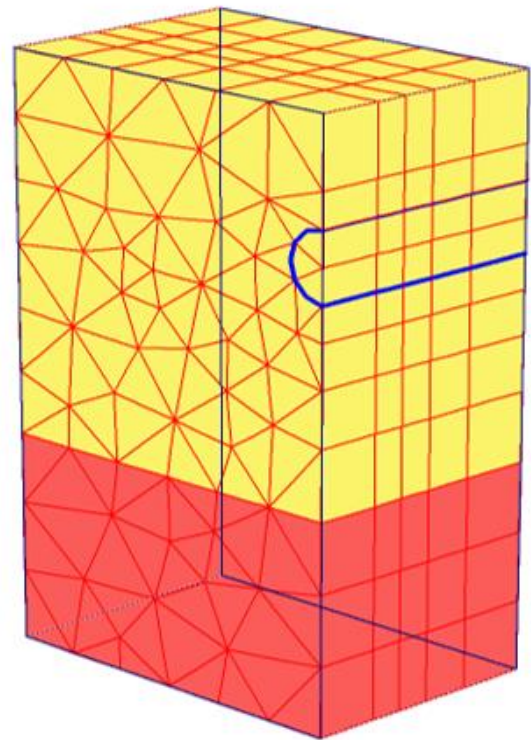
## III. RESULTS AND DISCUSSION

The results of ground movement are shown as in Fig. 2 and Fig. 3.

It can be seen that there is analogy between localized failure mechanism and local shear failure. The soil in front of the tunnel face is shifted forwards, whereas

the soil in regions located further away from the tunnel axis is forced outwards. This operation affects the ground and forms the failure areas. The funnel-shaped failure mechanism is similar to a five-block failure mechanism proposed by Soubra (2002) or the upper bound solutions for circular tunnel face by Davis et al. (1980). This model also adopted the study by Kovári and Anagnostou (1996). It consists of a wedge in front of the tunnel face and an overlying prismatic body, expanding to the surface in the state of limit equilibrium. At the same time, the pressure in front of the tunnel face is also formed. Therefore, the failure area depends on the C/D values, or the location of the tunnel.

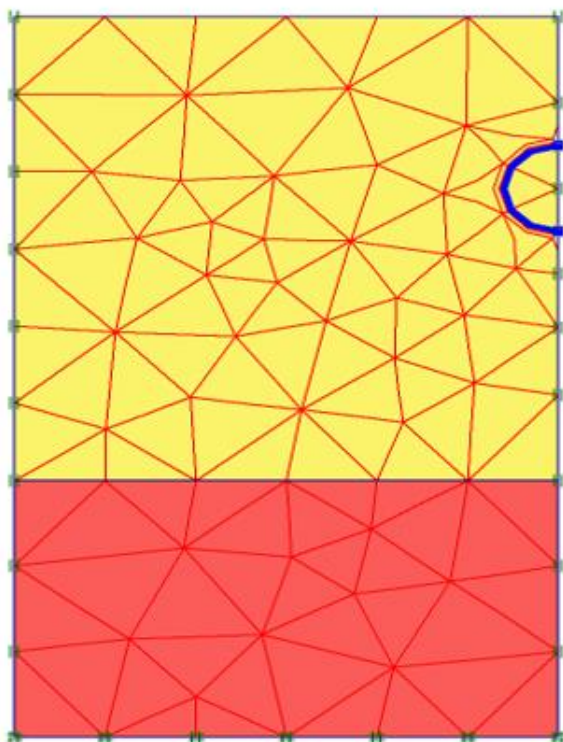
From Finite Element Method (FEM) result, sort out the required data at the coordinates of X at 30, Y at the tunnel crown and Z at shear zones. Results are synthesized in Table III.



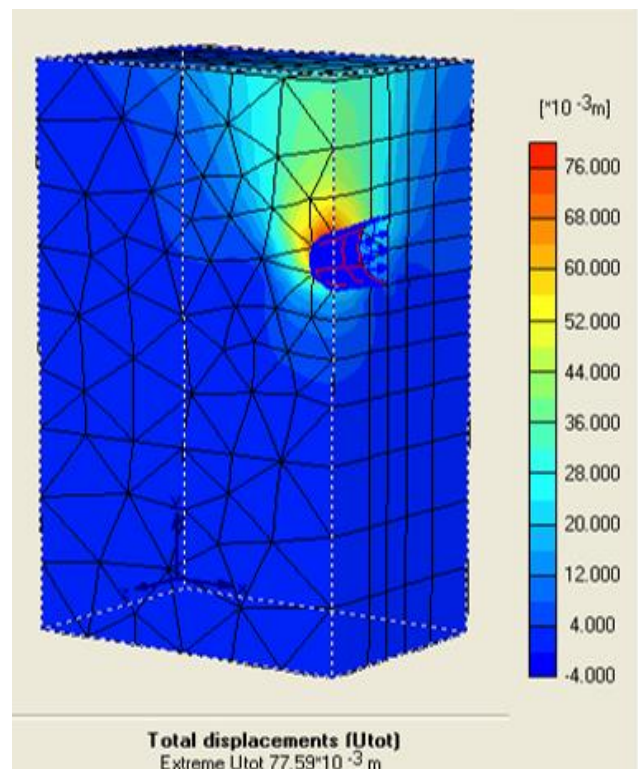
b)

**Figure 1.** Geometrical configuration of stability model

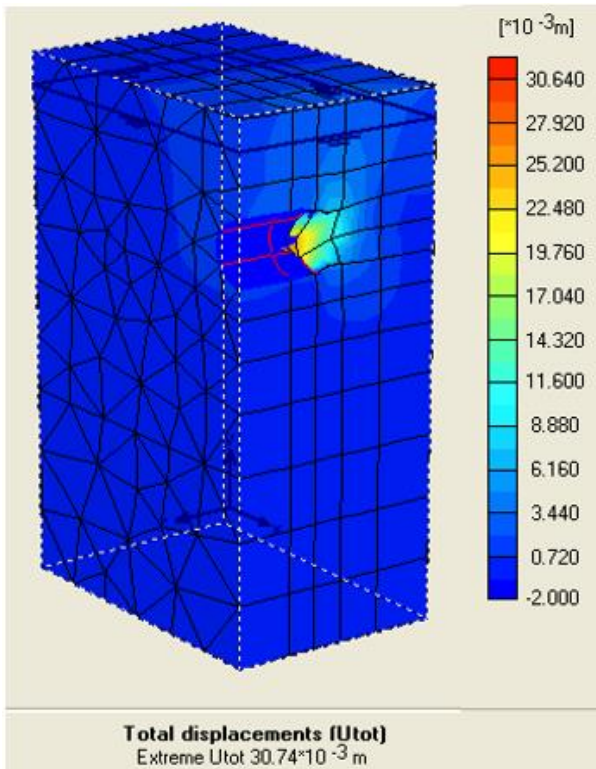
(a) 2D mesh (b) 3D mesh



a)



a)



b)

**Figure 2.** Displacement increments at the end of a) Phase 1 and b) Phase 2

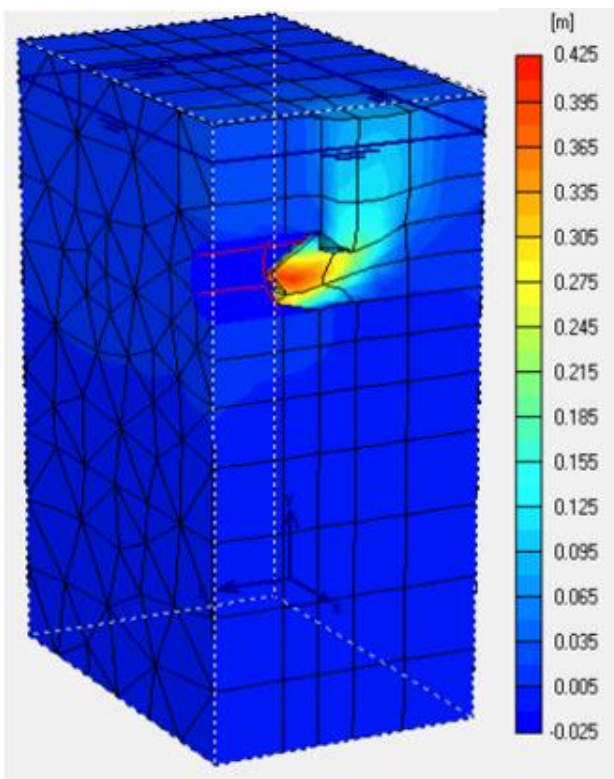


**Figure 3.** Ground deformation

**TABLE IIIII**

**TUNNEL MOVEMENT AT THE RATIO OF C/D = 1.5**

Node	X (m)	Y (m)	Z (m)	Ux (m)	Uy (m)	Uz (m)
957	30	-9	-7.8	0	0.0191	0.0044
964	30	-9	-7.8	0	0.0186	0.0001
1045	30	-9	-	0	-	-
1049	30	-9	9.1819	0	0.1511	0.0014
1308	30	-9	-	0	-	-
1315	30	-9	9.1819	0	0.1510	0.1409
1396	30	-9	-	0	-	-
1400	30	-9	10.563	0	0.2023	0.0253
1659	30	-9	-	0	-	-
1666	30	-9	10.563	0	0.1999	0.1707
			-	0	-	-
			12.518	0	0.1529	0.0513
			-	0	-	-
			12.518	0	0.1517	0.0887
			-	0	-	-
			14.472	0	0.0467	0.0349
			-	0	-	-
			14.472	0	0.0467	0.0330

From FEM results at different C/D ratios, we have a graph as shown in Fig. 4 and Fig.5.

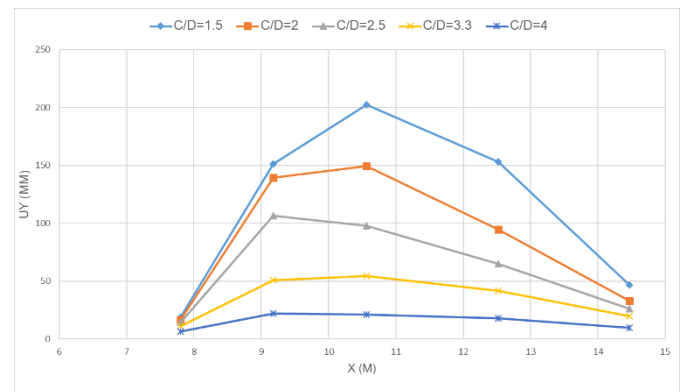


**Figure 4.** Tunnel deformation at different depths

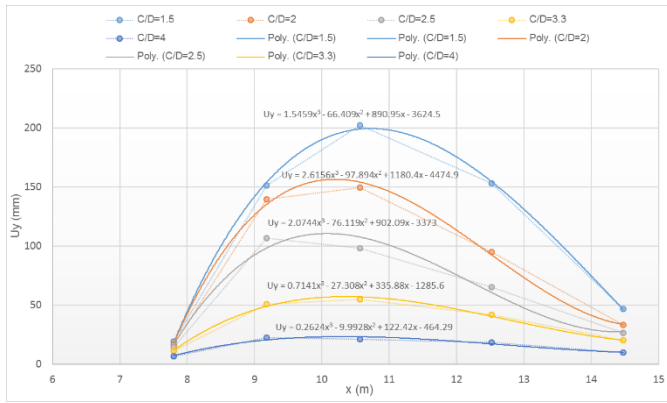


Figure 5. Equation of the tunnel settlement

From below equations of lines, the equation of the tunnel settlement subject to the depth in general form would be:

$$U_y = A_1 \cdot x^3 - A_2 \cdot x^2 + A_3 \cdot x - A_4 \quad (1)$$

In which:  $A_1, A_2, A_3, A_4$ : dependent variables on  $C$  and  $D$ .

Based on the coefficients of equations in Fig. 5,  $A_1, A_2, A_3$  and  $A_4$  are defined as in Table IV.

TABLE IVV  
COEFFICIENTS  $A_1, A_2, A_3$  VÀ  $A_4$

C/D	$A_1$	$A_2$	$A_3$	$A_4$
1.5	1.5459	-66.409	890.95	-3624.5
2	2.6156	-97.894	1180.4	-4474.9
2.5	2.0744	-76.119	902.09	-3373
3.3	0.7141	-27.308	335.88	-1285.6
4	0.2624	-9.9928	122.42	-464.29

Suggest the relation graphs between  $A_1, A_2, A_3, A_4$  and  $C/D$  as shown in Fig. 6 based on parameters.

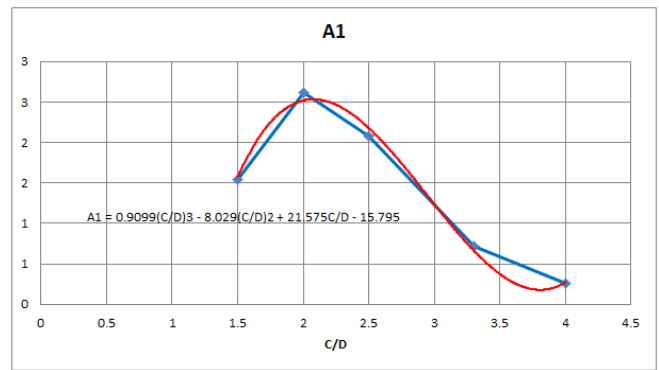
We have

$$A_1 = 0.9099(C/D)^3 - 8.029(C/D)^2 + 21.575C/D - 15.795 \quad (2)$$

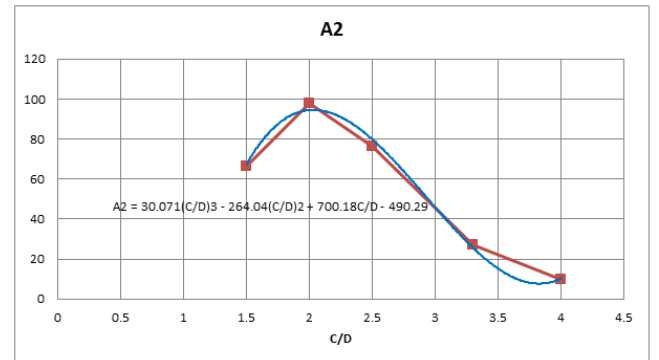
$$A_2 = 30.071(C/D)^3 - 264.04(C/D)^2 + 700.18C/D - 490.29 \quad (3)$$

$$A_3 = 320.35(C/D)^3 - 2797.3(C/D)^2 + 7306.8C/D - 4845.3 \quad (4)$$

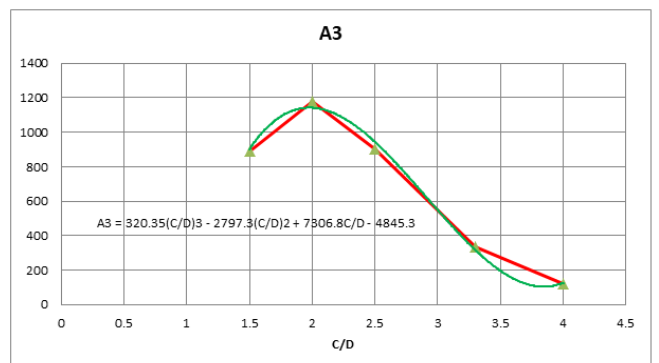
$$A_4 = 1100.5(C/D)^3 - 9559.8(C/D)^2 + 24618C/D - 15467 \quad (5)$$



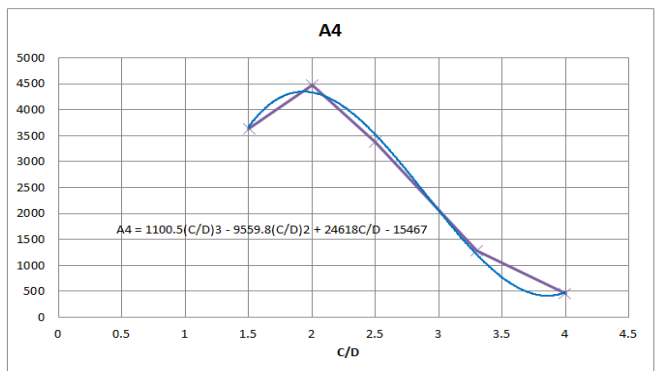
a)



b)



c)



d)

Figure 6. Relation graphs between  $A_1, A_2, A_3, A_4$  and  $C/D$

From the above diagrams, we find the coefficients  $A_1$ ,  $A_2$ ,  $A_3$  and  $A_4$  at different C/D ratios based on Equation 1.

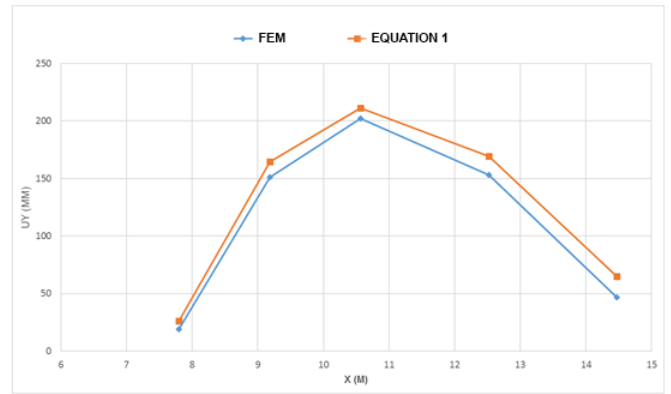
Table V. COMPARISON OF COEFFICIENTS  $A_1$ ,  $A_2$ ,  $A_3$  AND  $A_4$  DETERMINED BY EQUATION 1 AND NUMERICAL SIMULATION

C/D	$A_{1Equation}$	$A_{2Equation}$	$A_{3Equation}$	$A_{4Equation}$
1.5	1,5756	-67,38	902,76	-3663,6
2	2,5208	-94,478	1142,5	-4332,8
2.5	2,1806	-79,769	944,26	-3523,6
3.3	0,6655	-25,57	315,73	-1213,8
4	0,2701	-10,334	123,82	-479,2
C/D	$A_{1FEM}$	$A_{2FEM}$	$A_{3FEM}$	$A_{4FEM}$
1.5	1,5459	-66,409	890,95	-3624,5
2	2,6156	-97,894	1180,4	-4474,9
2.5	2,0744	-76,119	902,09	-3373
3.3	0,7141	-27,308	335,88	-1285,6
4	0,2624	-9,9928	122,42	-464,29

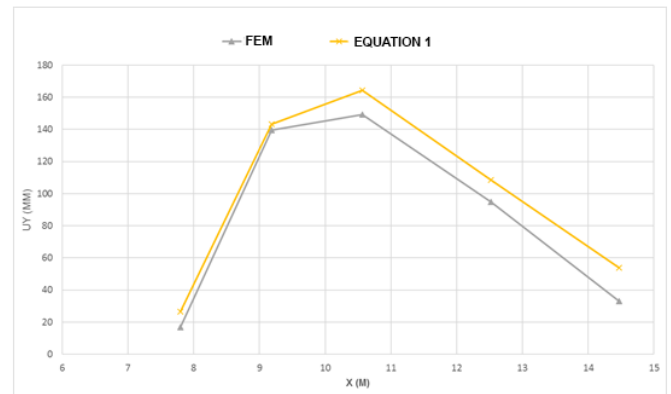
After making calculation, results as shown in Table VI.

Table VI. TUNNEL SETTLEMENT BY EQUATION 1

Formul a	x (m)	C/D			
		1.5	2.0	2.5	3.3
$U_y$ (mm)	7.8	26.255	26.578 1	23.257 7	9.0209 3
	9.181	164.54	143.29	109.34	44.637
	9	2	2	0	5
	10.56	211.25	164.36	120.16	52.614
	3	0	4	6	1
	12.51	169.43	108.43	74.083	37.183
	8	7	6	6	7
	14.47	64.923	53.939	44.196	17.355
	2	3		0	5



a)



b)

Figure 7. Deviation  $U_y$  (mm) between numerical stimulation and Equation (1): (a) C/D=1.5 (b) C/D=2.0

#### IV. CONCLUSION

From the results of the calculation, the following conclusions can be drawn

- ✓ There is analogy between localized failure mechanism and local shear failure. The failure area depends on the C/D values, or the location of the tunnel.
- ✓ The tunnel depth is larger, the largest tunnel settlement is smaller; therefore so sphere of influence on the ground construction will be reduced in direct proportion to the tunnel depth.
- ✓ It is critical to analyse the tunnel pressure in the construction process, the deeper the tunnel is, the greater the stress in front of tunnel is. As a result, it is necessary to calculate the minimum amount of a fluid (bentonite) to limit the

instability of the tunnel. In the case of minor errors, the proposed equation in this paper can be applied to determine the vertical and horizontal stresses in front of in sandy soils.

- ✓ The appropriate choice of model and input data plays an important role in the simulation results. These models should be carefully considered to show the relevant geological conditions, which helps to obtain realistic results of soil collapse in front of the tunnel.

## V. REFERENCES

- [1]. Anagnostou, G., & Kovari, K. 1994. The face stability of slurry-shield-driven tunnels. *Tunnelling and Underground Space Technology incorporating Trenchless*, 9(2), 165-174.
- [2]. Anagnostou, G., & Kovari, K. 1996. Face Stability Conditions with Earth-PressureBalanced Shields. *Tunnelling and Underground Space Technology*, 11(2), 165-173.
- [3]. Atkinson, J. H., Brown, E. T. and Potts, D. M. 1975. Collapse of shallow unlined tunnels in dense sand. *Tunnels and Tunnelling*, Vol. 3, pp. 81-87.
- [4]. Broms, B. B. and Bennermark, H. 1967. Stability of clay at vertical openings. *ASCE Journal of Soil Mechanics and Foundation Engineering Division SM1*, Vol. 93, pp. 71-94.
- [5]. R. B. J. Brinkgreve and P. A. Vermeer. 2001. "PLAXIS Finite Element Code for Soil and Rock Analyses". A. A. Balkema, Rotterdam.
- [6]. Davis, E. H., Gunn, M. J., Mair, R. J., & Seneviratne, H. N. 1980. The stability of shallow tunnels and underground openings in cohesive material. *Geotechnique*, 30(4), 397-416.
- [7]. Dias, D., Janin, J. P., Soubra, A. H., & Kastner, R. 2008. Three-dimensional face stability analysis of circular tunnels by numerical simulations. In *Geotechnical Special Publication*, (eds), pp. 886-893.
- [8]. Kovari K., Anagnostou G. 1996. Face stability in slurry and EPB shield tunnelling. *Proc Int. Symp. on Geotechnical Aspects of Underground Construction in Soft Ground*, City University, Balkema, 453-458.
- [9]. Leca, E., & Dormieux, L. 1990. Upper and lower bound solutions for the face stability of shallow circular tunnels in frictional material. *Geotechnique*, 40(4), 581-606.
- [10]. Loganathan N, Poulos HG. 1998. Analytical prediction for tuinnelling – induced ground movements in clays, *J of Geotech. and Geenviron. Eng. ASCE*, 124 (9), 846-856.
- [11]. Mollon, G., Dias, D., Soubra, A. H. 2010. Face Stability Analysis of Circular Tunnels Driven by a Pressurized Shield", *Journal of Geotechnical and GeoEnvironmental Engineering*, 136(1), 215-229.
- [12]. Soubra, A. H. 2002. Kinematical approach to the face stability analysis of shallow circular tunnels. *Proceedings of the Eight International Symposium on Plasticity*, 443-445.
- [13]. Soubra, A. H., Dias, D., Emeriault, F., & Kastner, R. 2008. Three-dimensional face stability analysis of circular tunnels by a kinematical approach. *Geotechnical Special Publication*, 894-901.
- [14]. Vermeer, P. A., Nico Ruse and Thomas Marcher. 2002. Tunnel Heading Stability in Drained Ground. *FELSBAU 20*, pp. 8-18.
- [15]. Verruijt, A. and Booker, J. R. 1996. Surface settlements due to deformation of a tunnel in an elastic half plane. *Géotechnique*, Vol. 46, No. 4, pp. 753-756.
- [16]. WONG Kwong Soon. 2012. Passive failure and deformation mechanisms due to tunnelling in sand and clay, PhD. Thesis, The Hong Kong University of Science and Technology.

- [17]. WONG Kwong Soon, C.W.W. Ng, Y.M. Chen, X.C. Bian. 2012. Centrifuge and numerical investigation of passive failure of tunnel face in sand. *Tunnelling and Underground Space Technology* 28, pp. 297-303.

**Cite this article as :**

Tuan Anh Nguyen, Minh Anh Trong Nguyen, "Study on Tunnel Face Failure Mechanism in Two-Layer Soils", *International Journal of Scientific Research in Civil Engineering (IJSRCE)*, ISSN : 2456-6667, Volume 5 Issue 2, pp. 09-16, March-April 2021. URL : <https://ijsrce.com/IJSRCE21525>